Supplementary materials and methods

Characterizing and minimizing the contribution of sensory inputs to TMS-evoked potentials

Mana Biabani [a], Alex Fornito [a], Tuomas P. Mutanen [b], James Morrow [a], Nigel C. Rogasch [a]

[a] Brain and Mental Health Research Hub, Monash Institute of Cognitive and Clinical Neuroscience, School of Psychological Sciences, Monash Biomedical Imaging, Monash University, VIC, Australia

[b] Centre for Cognitive Neuroimaging, Institute of Neuroscience and Psychology, University of Glasgow, Glasgow G12 8QB, United Kingdom

Supplementary methods

EMG

EMG signals were amplified (x1000), band-pass filtered (10-1000 Hz), digitized at 5 kHz and epoched around the TMS pulse (-200 to 500ms). The signals were displayed online on a computer screen.

EEG

EEG signals were amplified (x1000), low pass filtered (DC – 2000 Hz), digitized at 10 kHz and recorded on a computer using the Curry8 software (Neuroscan, Compumedics, Australia), for offline analysis. The skin-electrode impedance level was maintained at below 5 kΩ throughout the session [1].

TMS

In experiment I, the stimulator was set to deliver biphasic pulses with anterior-posterior and then posterior-anterior direction in the underlying cortex. For scalp stimulations, the TMS coil was held tangentially over the left side of the scalp with the handle pointing backward with an angle of 45° with the sagittal plane. For shoulder stimulation, the orientation and angle of the coil was changed until the participants reported the same level of local sensations under the coil between the real TMS and control conditions. We decreased the intensity for two participants since they reported propagation of the pulses towards the arm and hand, which couldn't be prevented by changing the coil orientation. One subject, however, did not feel a strong enough tapping sensation on the shoulder so we increased the intensity to 135% rMT. On average, the stimulation intensity used for control conditions was not significantly different from 120% rMT ($p = 0.8$) (supplementary table. 1).

In experiment II, monophasic TMS was delivered in the posterior-anterior direction through a figure-of-eight-shaped coil (7 cm wing diameter), connected to a Magstim 200 stimulator (Magstim Company, UK). This session was a part of a larger experiment in which the number of pulses was reduced (to an average of 75 pulses) to prevent the coil from overheating. Again, for this condition, the stimulation intensity used for control conditions was not significantly different from 120% rMT ($p = 0.11$) (supplementary table. 1).

In all of the conditions, TMS pulses were given with the intervals jittered between 4 and 6 s and the order of the real TMS and control conditions was pseudorandomized within each session.

EEG analysis

First, the responses to the different stimulation conditions were concatenated together and epoched with a window of -1000 ms to 1000 ms around the TMS pulse, and the mean of each channel's baseline (defined as a window of -500 to -10ms) was removed from each epoch. The TMS pulse artifact (the data from -2 to 15ms) was then removed and a cubic interpolation was applied to replace the missing data. The recordings were then down sampled to 1000 Hz. Following which, the trials and channels affected by prominent artefacts were detected by visual inspections and removed (supplementary table. 1). Afterwards, the interpolated data around TMS pulse were replaced with constant amplitude data and the TMS induced muscle and decay artifacts were identified using the FastICA algorithm [2] and rejected. A linear interpolation was applied to replace the missing data. Data were then band-pass (1-100 Hz) and band-

stop (48-52 Hz) filtered using a zero-phase Butterworth filter (order = 4) and other artifacts such as blinks and noise-related artefacts were corrected by applying a second run of FastICA algorithm. Artifactual components were selected using the TESA automated functions with default settings and checked visually (supplementary table. 1). Finally, the rejected channels were spatially interpolated using spherical method and all data were re-referenced to the common average. TEPs and SEPs were computed for each participant and each condition by averaging the recordings over trials.

Supplementary table 1. The average of rMT, stimulation intensities, and preprocessing outputs for each condition.

	Experiment I			**Experiment II**	
	120% rMT M1	**80% rMT M1**	**120% rMT Shoulder**	**120% rMT M1**	**120% rMT Shoulder**
rMT (mean ± SD)	56.8 ± 8.5	56.8 ± 8.5	56.8 ± 8.5	47.8 ± 6.6	47.8 ± 6.6
Intensity (mean ± SD)	68.2 ± 10.3	45.7 ± 6.9	67.9 ± 9.9	57.0 ± 7.9	55.6 ± 8.3
Remaining trials (mean ± SD)	78.0 ± 12.0	82.4 ± 9.5	81.4 ± 15.5	69.5 ± 23.5	70.2 ± 22.6
Remaining channels (mean ± SD)	61.6 ± 0.9	61.6 ± 0.9	61.6 ± 0.9	61.1 ± 1.2	61.1 ± 1.2
ICs removed (mean ± SD)	23.6 ± 4.9	23.6 ± 4.9	23.6 ± 4.9	23.3 ± 6.9	23.3 ± 6.9

rMT = Resting motor threshold; M1 = Primary motor cortex; ICs = Independent components

Source estimation

First, each individual's T1 scan was automatically segmented using FreeSurfer software (version 5.3). After visual inspections and manual corrections, the FreeSurfer output was imported to Brainstorm and the cortical surface was down sampled to 15,000 vertices. Registration between EEG and MRI was then performed by aligning the locations of EEG electrodes with the generated surfaces. Afterwards, the head model was computed using a three-layer symmetric Boundary Element Method (BEM; OpenMEEG freeware), applying the default conductivity values (i.e. scalp = 1, skull= 0.0125 and brain= 1) [3]. The noise covariance matrix (Depth weighting: 0.5, Regularize noise covariance: 0.1, SNR: 3) was then calculated following concatenation of the baseline periods (-1s to -0.002s pre-stimulus), for each trial, each individual and each condition separately. Afterwards, cortical sources were estimated using minimum norm estimation (MNE), for which, sources were constrained to be normal to the surface of the cortex [4]. The source amplitude was then transformed into z-score relative to the baseline for each individual at each condition, and then projected to a common default anatomy (ICBM152) to facilitate averaging across participants and group analyses. The source values where then smoothed with the kernel size of 3mm for display purposes.

Source estimation was also performed using dipole fitting method for one selected point of time. For this method, 15000 freely oriented dipoles were positioned on the cortical surface. Dipole fitting was performed by minimizing the sum of squared errors between the scalp measured and projected data, and the dipole with the highest goodness of fit (GOF; i.e. the least error) was defined as the most likely location of the cortical source [5]. The dipole fit was considered reliable if GOF value was over 0.90

[6]. The individuals' selected dipoles were then projected to the default anatomy for group analyses.

Supplementary results

Effect of stimulation parameters

TMS-EEG studies are performed using a variety of different stimulation parameters, including different intensities, and pulse waveforms. To assess whether the relationship between TEPs and SEPs generalises between other parameter choices, we repeated the analyses on two different data sets:

1) Biphasic pulses and a subthreshold intensity (Supplementary Fig. 1-3).

2) Monophasic pulses and a suprathreshold intensity (Supplementary Fig. 4-7), for which, the same type of pulses was applied over shoulder as control condition. All of the assessments performed for biphasic stimulations were repeated for this condition.

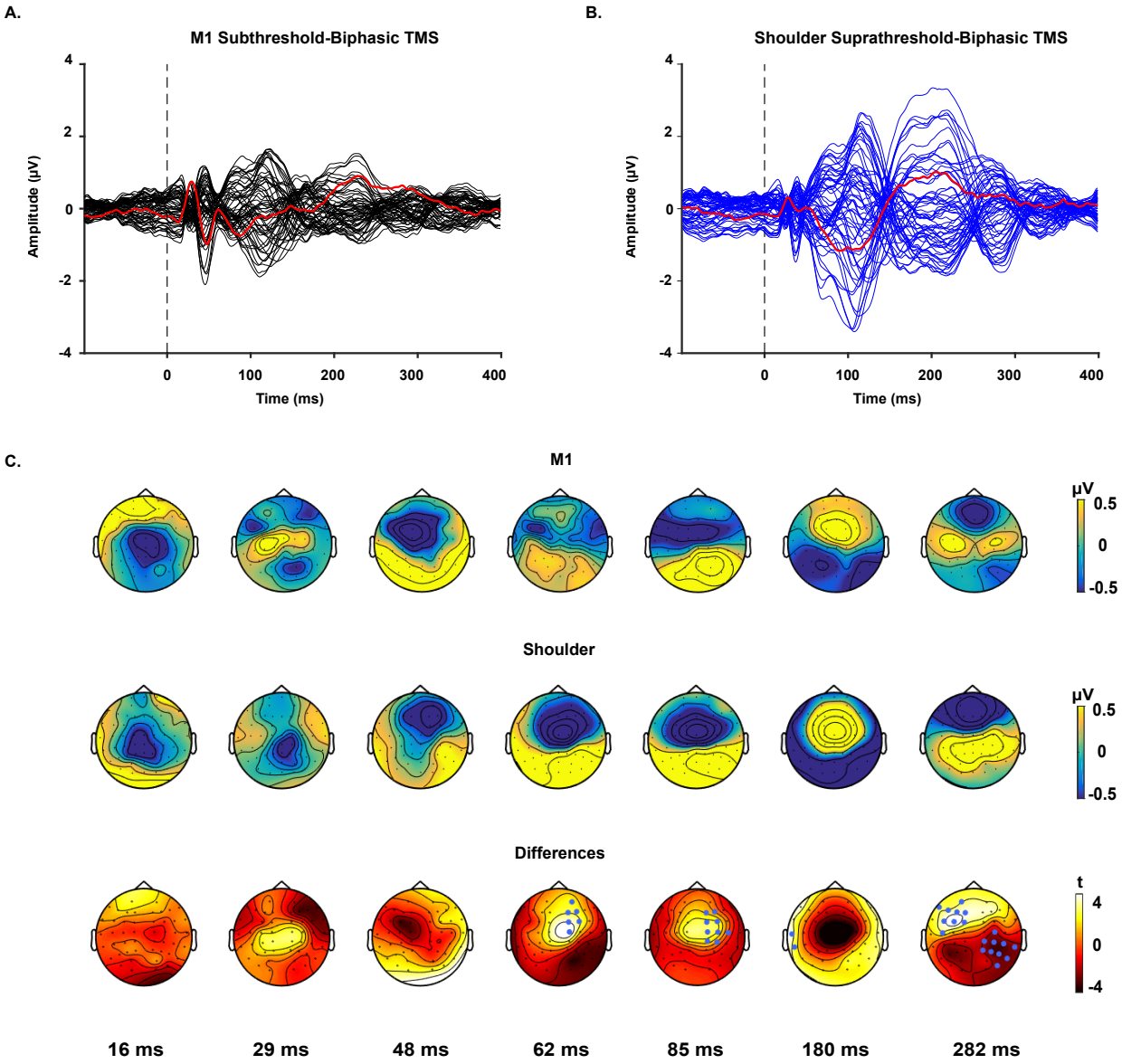

Supplementary Fig. 1 TMS-evoked potentials following subthreshold, biphasic stimulation over left M1 and suprathreshold, biphasic stimulation over left shoulder. The butterfly plots demonstrate the grand-average of potentials recorded by each electrode. A) Responses to the stimulation of M1. B) Responses to the stimulation of shoulder. The red lines indicate the recordings by the electrode underneath the coil (C3). The vertical dash line indicates the point of time when TMS is applied. C) The upper and middle topoplots depict voltage distributions across the scalp for each peak of interest, in response to the real and control conditions, respectively. The lower topoplots illustrate the results of the cluster-based permutation tests comparing the

voltage distribution of the two responses at each peak. Clusters were defined as at least two neighbouring electrodes exceeding the threshold of p-value < 0.05 at each point of time. Monte Carlo p-values were calculated on 5000 iterations with a critical α level set at $p<0.025$. The channels highlighted by blue dots belong to the clusters that showed statistically stronger responses to shoulder stimulation ($p<0.025$). One negative and two positive significant clusters were found.

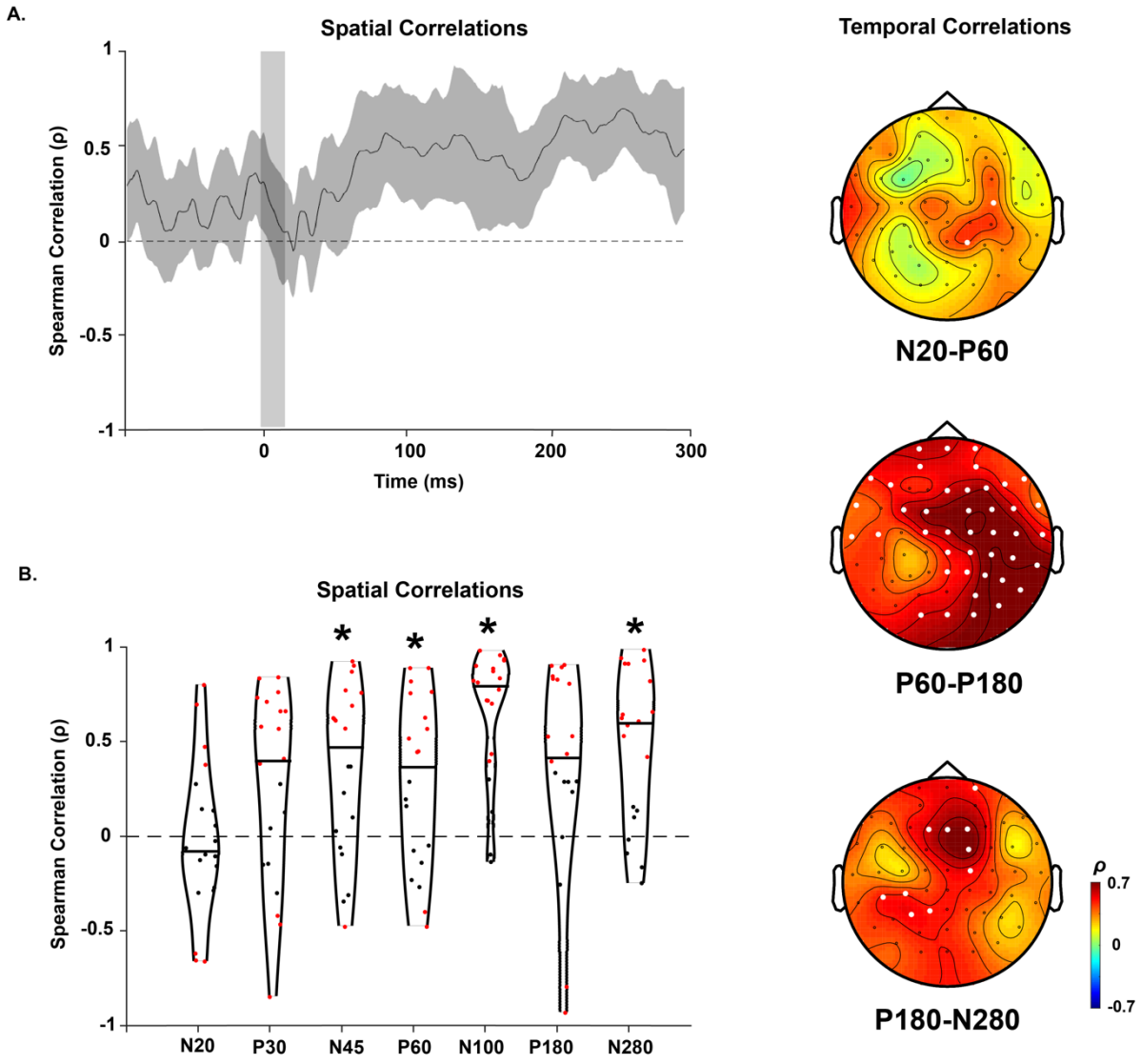

Supplementary Fig. 2 Spatiotemporal correlations of subthreshold TEPs and suprathreshold SEPs. A) The spatial correlations of the potentials at each point of time from 100 ms before to 300 ms following stimulations. The grey shaded area represents the 95% CIs. The vertical grey bar shows the window of interpolated potentials around stimulus. B) The distribution of spatial correlations across individuals. The dots within the violin plots represent the correlation values at for each individual. The red dots show significant positive and negative correlations respectively ($p<0.05$) and the black dots represent non-significant correlations. * indicates that correlation values differed from 0 at the group level (one-sample t-test, $p<0.05$). C) The temporal correlations of

the potentials at each window of time. White dots indicate the electrodes with significant positive correlations ($p<0.05$). No significant negative correlation was found.

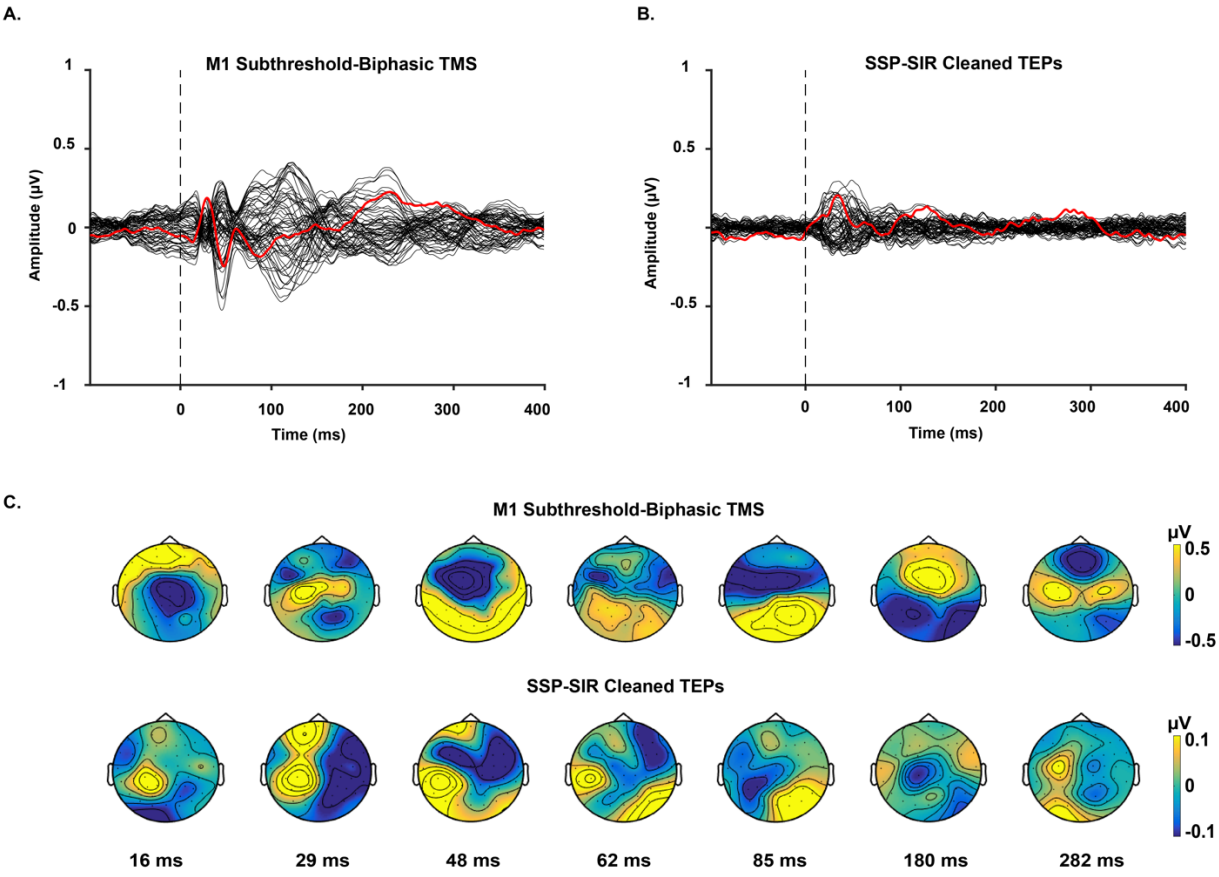

Supplementary Fig. 3 TMS-evoked potentials following subthreshold, biphasic stimulation over left M1 before and after applying SSP-SIR. The butterfly plots demonstrate the grand-average of potentials recorded by each electrode before (A) and after (B) applying SSP-SIR. The red lines indicate the recordings by the electrode underneath the coil (C3). The vertical dash line indicates the point of time when TMS is applied. C) Voltage distributions across the scalp for each peak of interest before (upper plots) and after SSP-SIR (lower).

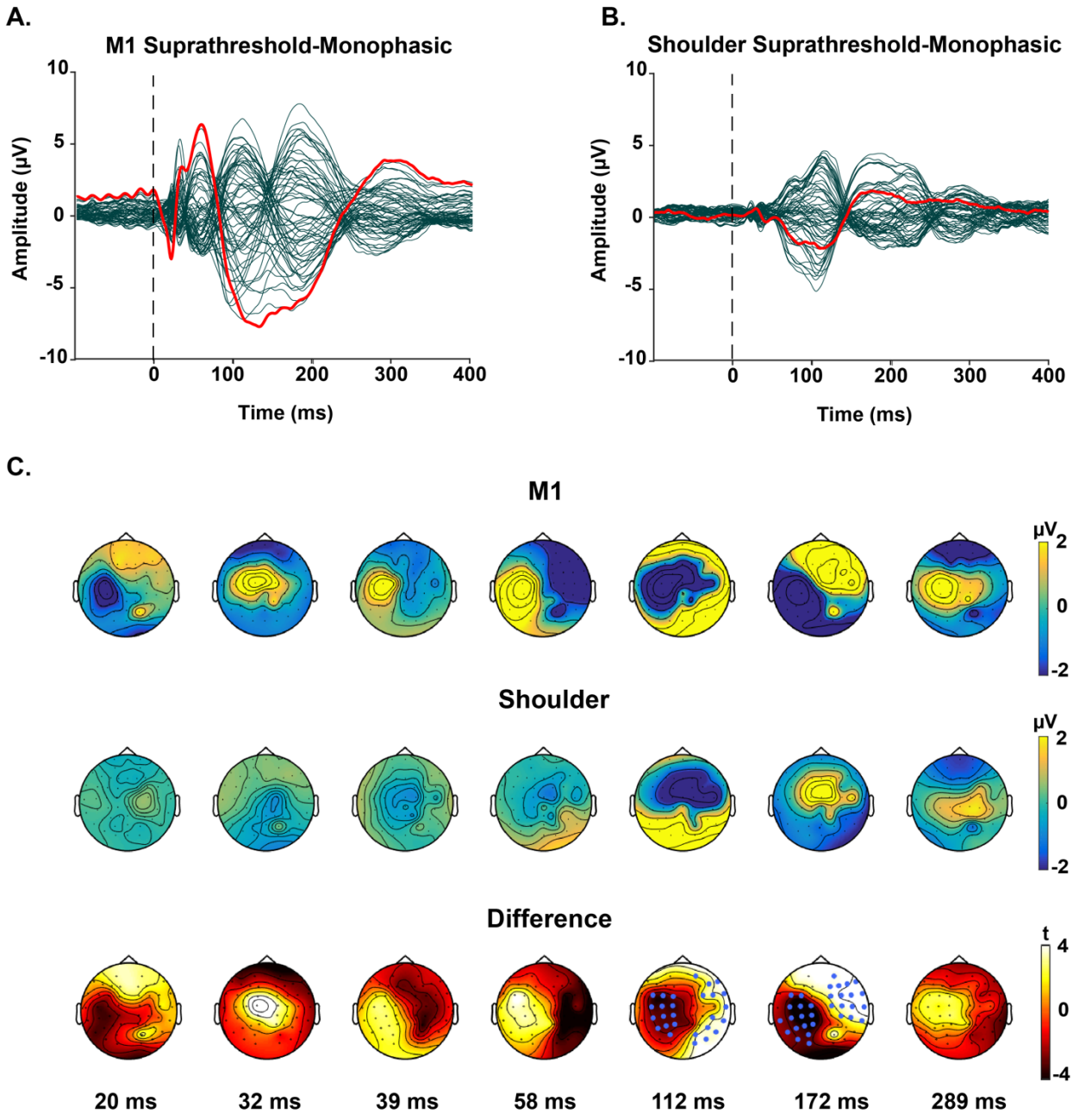

Supplementary Fig. 4 TMS-evoked potentials following suprathreshold, monophasic stimulations over left M1 and left shoulder. The butterfly plots demonstrate the grand-average of potentials recorded by each electrode. The red lines indicate the recordings by the electrode underneath the coil (C3). The vertical dash indicates the point of time when TMS is applied. A) Responses to the stimulation of M1. B) Responses to the stimulation of shoulder. C) The upper and middle topoplots depict voltage distributions across the scalp for each peak of interest, in response to the real and control

conditions, respectively. The lower topoplots illustrate the results of the cluster-based permutation tests comparing the voltage distribution of the two responses at each peak. Clusters were defined as at least two neighbouring electrodes exceeding the threshold of p-value < 0.05 at each point of time. Monte Carlo p-values were calculated on 5000 iterations with a critical α level set at $p<0.025$. The channels highlighted by blue dots belong to the clusters that showed statistically stronger responses to the real TMS condition ($p<0.025$). Three negative and two positive significant clusters were found.

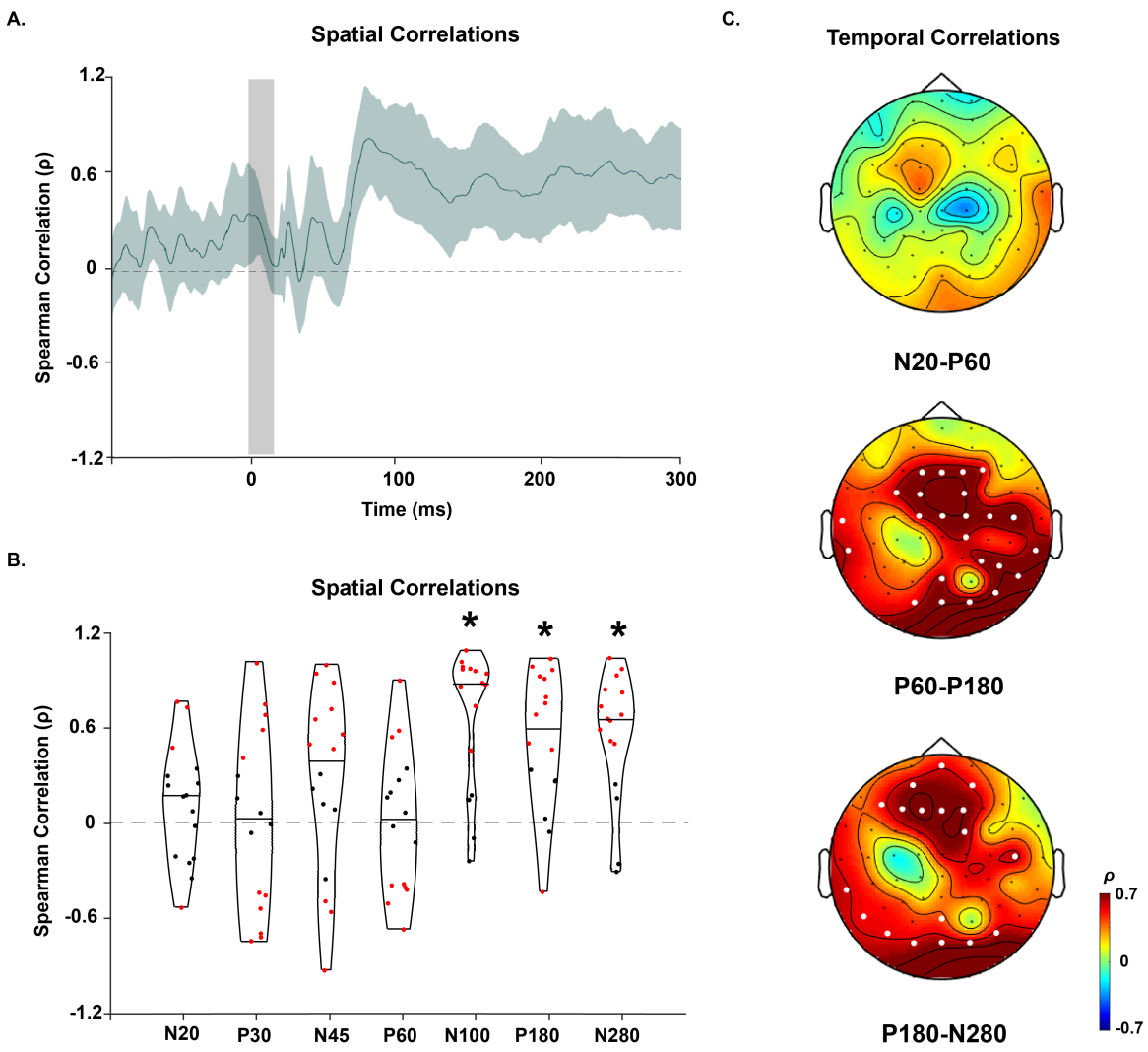

Supplementary Fig. 5 Spatiotemporal correlations of TEPs and SEPs evoked by suprathreshold, monophasic TMS. A) The spatial correlations of the potentials at each point of time from 100 ms before to 300 ms following stimulations. The green shaded area represents the 95% CIs. The vertical grey bar shows the window of interpolated potentials around stimulus. B) The distribution of spatial correlations across individuals. The dots within the violin plots represent the correlation values at for each individual. The red dots show significant positive and negative correlations respectively ($p<0.05$) and the black dots represent non-significant correlations. * indicates that correlation values differed from 0 at the group level (one-sample t-test, $p<0.05$). C) The temporal correlations of the potentials at each window of time. White

dots indicate the electrodes with significant positive correlations ($p<0.05$). No significant negative correlation was found.

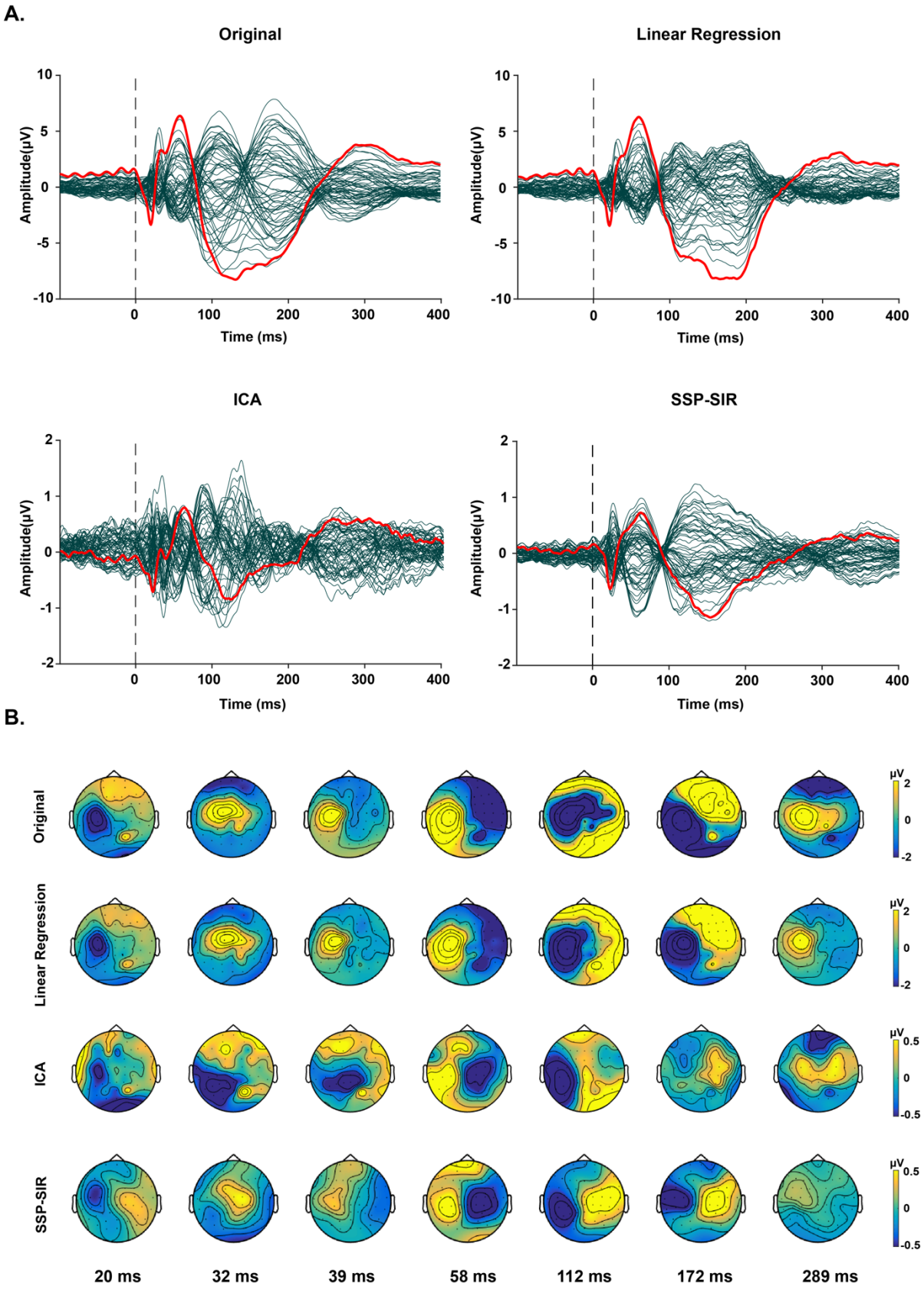

Supplementary Fig. 6 The alterations in the spatiotemporal distributions of TEPs induced by suprathreshold and monophasic TMS before and after removing SEPs

using three different filtering methods. A) The butterfly plots demonstrate the grand-average of the potentials recorded by each electrode before (original) and after employing each filtering method. The red lines indicate the recordings by the electrode underneath the coil (C3). The vertical dash line indicates the point of time when TMS is applied. B). The topoplots depict voltage distributions across the scalp for each peak of interest before (original) and after applying each filter.

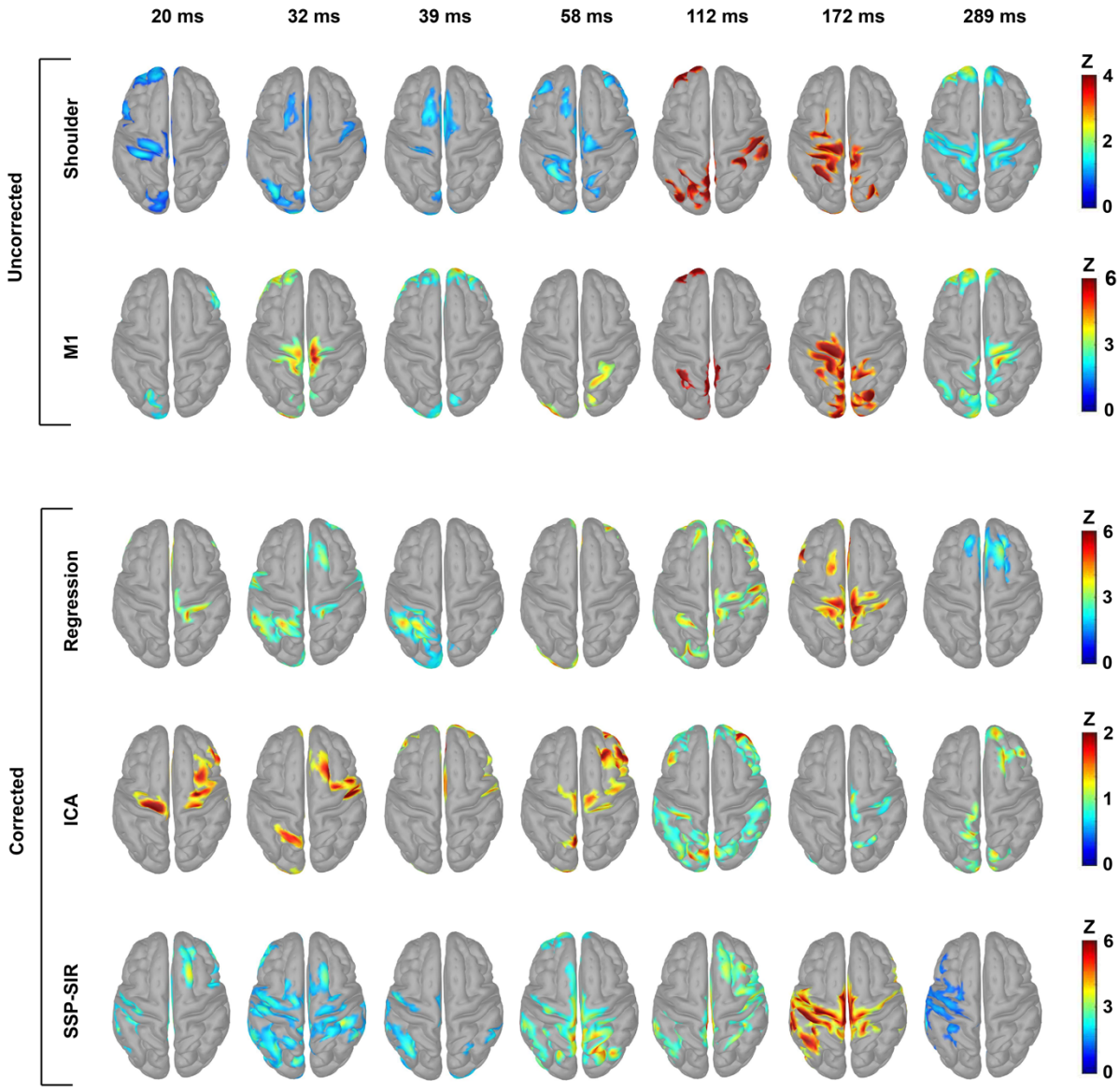

Supplementary Fig. 7 The estimated source distributions obtained by applying MNE to the TEPs (evoked by suprathreshold and monophasic TMS) from different filtering methods. MNE maps are thresholded at 40% of the maximum activity at each point of time and the minimum size for the activated regions is set to 50 vertices.

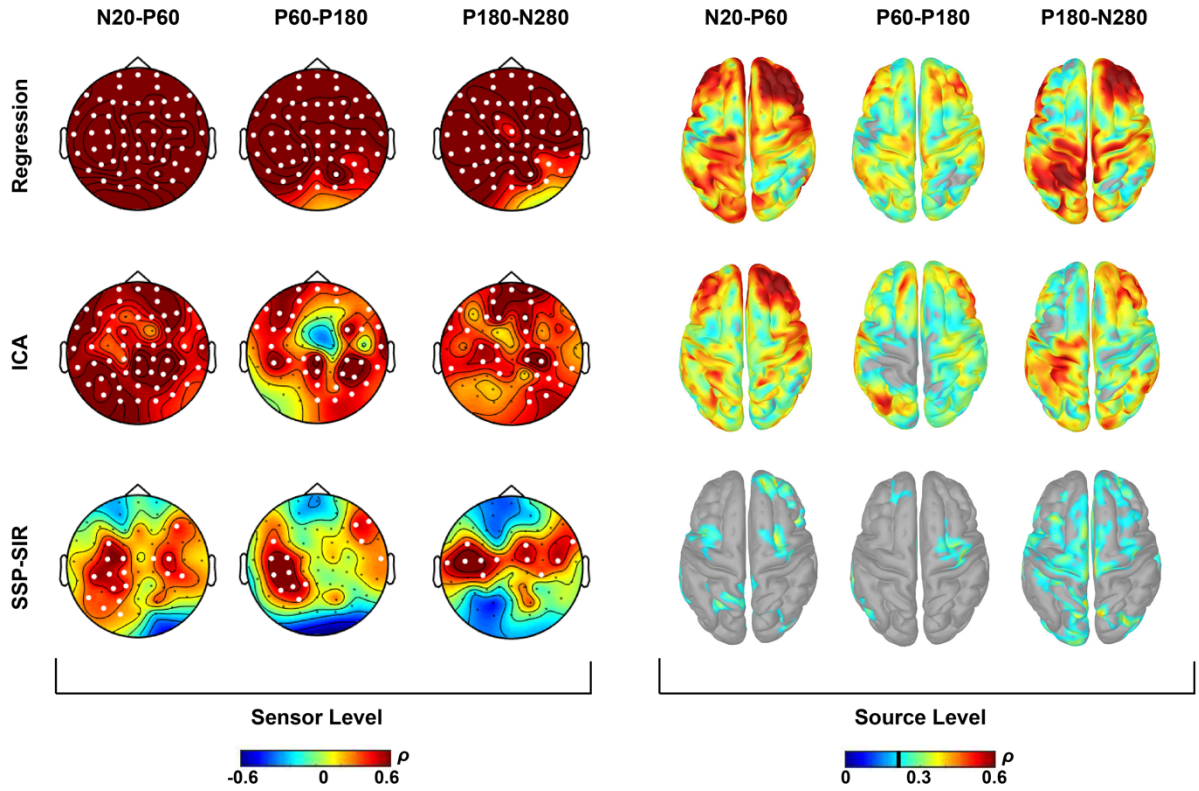

Supplementary Fig. 8 Spearman correlation measures between the original and filtered TEPs (evoked by suprathreshold and monophasic TMS) at both sensor and source levels, at three different intervals. The maps show the average of the correlation values at individualized time windows (i.e. N20-P60, P60-P180, P180-N280). A) The correlations between the original and filtered potentials recorded by each channel at each window of time. White dots indicate the electrodes with significant positive correlations ($p<0.05$). B) The distribution of the correlations between the estimated source activities at each vertex. The source maps are thresholded at $\rho>0.2$. Linear regression filtered data showed significant correlations with the original signal across the whole time and space domains. ICA, also, showed strong widespread correlations across time at both source and sensor levels. SSP-SIR resulted in substantially lower correlations (high suppression) especially around the fronto-central regions, which had shown sensory high contamination, but caused

minimum suppression to the recordings around the site of stimulation especially noticeable at the scalp level.

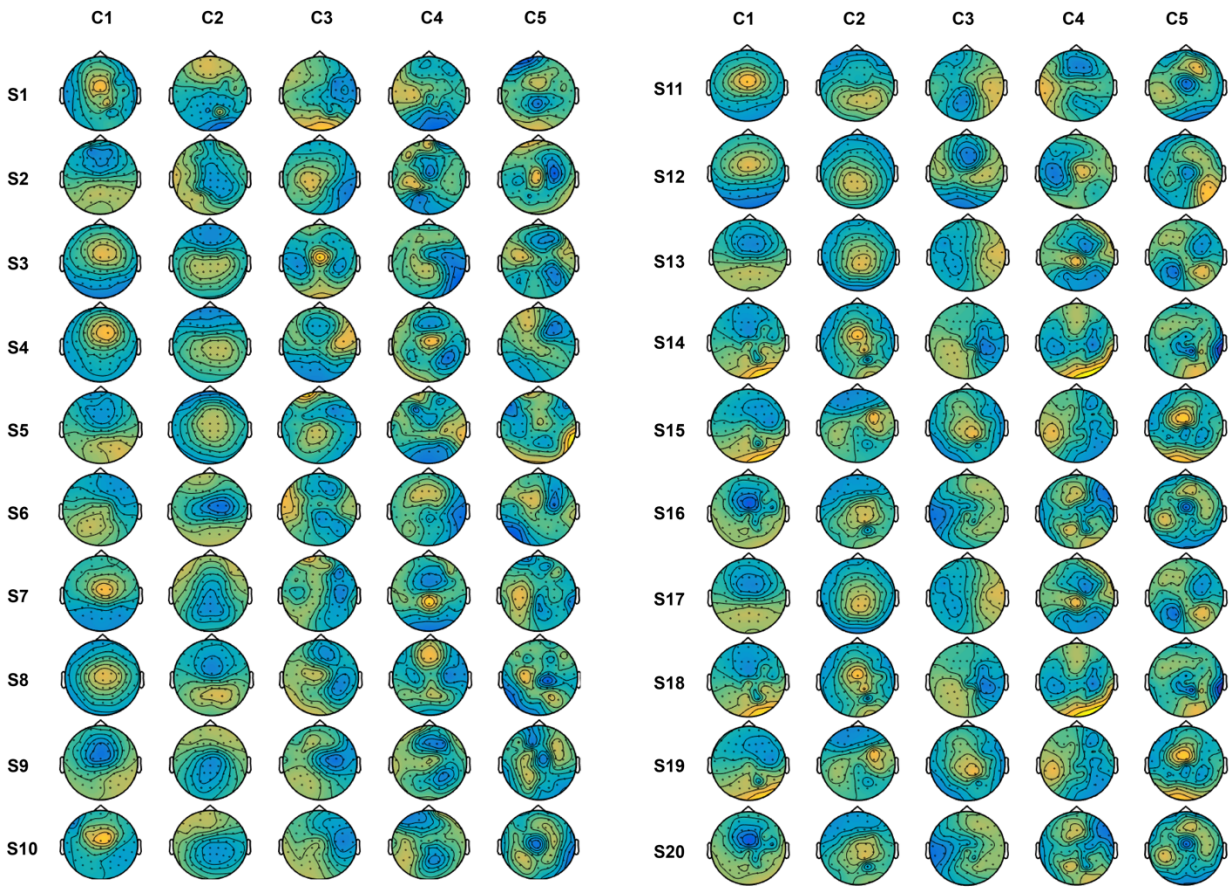

Supplementary Fig. 9 Topography of the first five artifactual components (C) rejected by SSP-SIR, for each subject (S) at biphasic and suprathreshold stimulation condition.

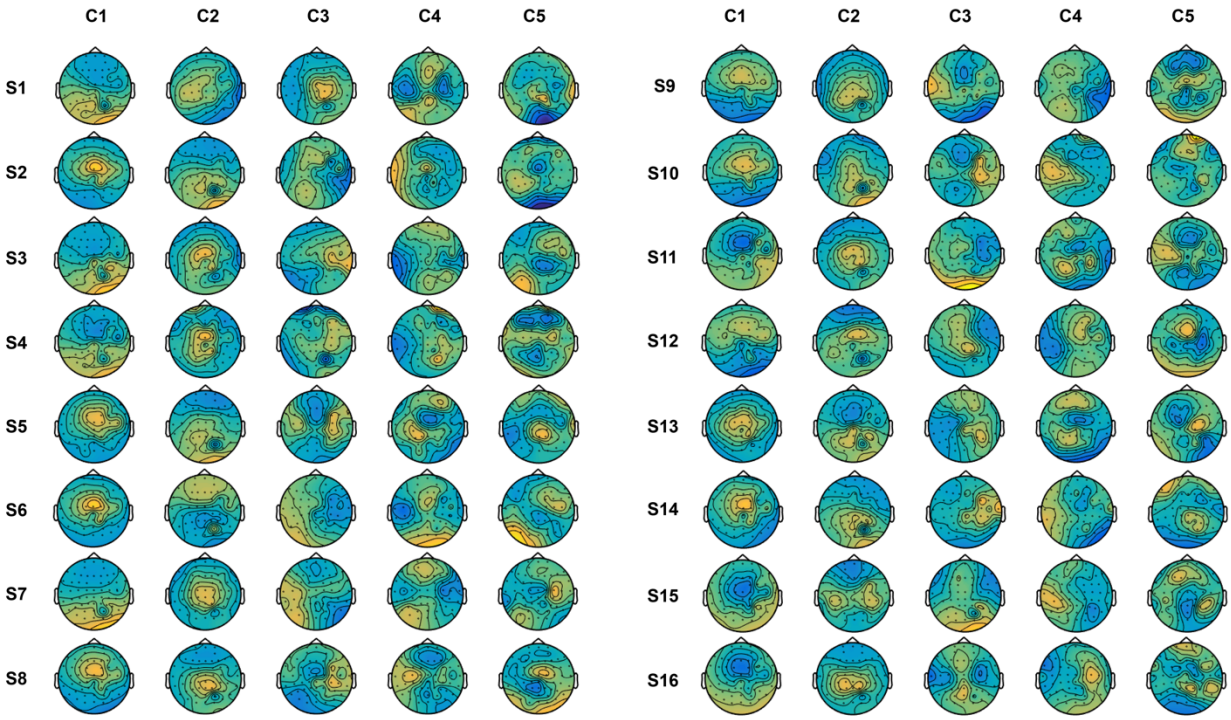

Supplementary Fig. 10 Topography of the first five artifactual components (C) rejected by SSP-SIR, for each subject (S) at monophasic and suprathreshold stimulation condition.

Supplementary references

[1] Ilmoniemi RJ, Kičić D. Methodology for combined TMS and EEG. Brain topography 2010;22(4):233.
[2] Hyvärinen A, Oja E. Independent component analysis: algorithms and applications. Neural networks 2000;13(4-5):411-30.
[3] Gramfort A, Papadopoulo T, Olivi E, Clerc M. OpenMEEG: opensource software for quasistatic bioelectromagnetics. Biomedical engineering online 2010;9(1):45.
[4] Lin FH, Belliveau JW, Dale AM, Hämäläinen MS. Distributed current estimates using cortical orientation constraints. Human brain mapping 2006;27(1):1-13.
[5] Kaukoranta E, Hämäläinen M, Sarvas J, Hari R. Mixed and sensory nerve stimulations activate different cytoarchitectonic areas in the human primary somatosensory cortex SI. Experimental brain research 1986;63(1):60-6.
[6] Mutanen TP, Metsomaa J, Liljander S, Ilmoniemi RJ. Automatic and robust noise suppression in EEG and MEG: The SOUND algorithm. NeuroImage 2018;166:135-51.